SPARSE EMISSION PATTERN IN SPECTRAL BLOOD DOPPLER

Regev Cohen and Yonina C. Eldar

Technion — Israel Institute of Technology, Haifa, Israel

ABSTRACT

Spectral Doppler ultrasound imaging allows quantification of blood flow by estimating the velocity distribution of the blood within a range gate on a single image line. In applications, it is desirable to have both brightness mode (B-mode) at high frame rate, to allow the medical doctor to visualize and follow vessel movement, as well as Doppler mode with high spectral resolution of the velocity distribution, so that changes in blood flow can be tracked. In this paper, we propose a slow-time sparse emission pattern of the blood Doppler signal which significantly reduces the number of transmissions sent. For the proposed sampling scheme, we derive the minimal number of Doppler emissions allowing reconstruction of the signal's power spectrum and provide power spectrum recovery techniques that achieve this minimal rate. Using realistic Field II simulations, we show that accurate estimation of blood velocity spectrum can be performed from only 12% of the transmissions required in conventional scanning. Thus, several vessel regions may be investigated while keeping a high frame rate of the B-mode images.

Index Terms— Ultrasound, Spectral Estimation, Nested Arrays, Blood Velocity Estimation , Blood Doppler.

1. INTRODUCTION

Spectral Doppler is a non-invasive technique commonly used in medical ultrasound. It enables quantitative estimation of local blood velocities in a chosen spatial region within a specific blood vessel. The data for velocity estimation is acquired by transmitting a train of narrowband ultrasound pulses along a desired direction at a constant pulse repetition frequency (PRF). The backscattered signals from each pulse emission are then sampled and focused along the chosen direction using dynamic focusing. Assembling the samples associated with a specific depth of interest from all emissions forms the so-called slow-time signal with a frequency proportional to the blood velocity along the direction of the ultrasound beam. The blood velocity distribution is then estimated by reconstructing the power spectral density (PSD) of the slow-time signal. The time needed for each velocity estimation is the coherent processing interval (CPI), which is equal to the number of transmitted pulses P divided by the PRF. Displaying spectral analysis results over time, referred to as a spectogram, visualizes changes in the blood velocity distribution.

In conventional commercial ultrasound systems, the spectogram is estimated using Welch's method [1], a modified averaged periodogram based on the fast Fourier transform (FFT) algorithm. However, this approach suffers from high leakage and requires a long observation window (OW), meaning that a large number of transmissions in the same direction has to be used in order to attain sufficient spectral resolution. As the number of transmitted pulses per unit of time is limited by the speed of sound and the desired depth being examined, there is an inherent trade off between spectral and temporal resolution. Furthermore, it is also important to update the B-mode image frequently to allow the medical doctor to examine the surrounding tissue of the vessel and navigate to choose the region in which the blood velocity is estimated. Conventionally, an interleaved B-mode/Doppler sequence is used where every second transmission is a B-mode acquisition, thereby halving the PRF. This results in reduction of the maximal velocity that can be measured by a factor of two, according to the Nyquist theorem. An alternative approach is to use a block of B-mode transmissions, but this results in holes in the blood velocity spectogram. These limitations raise the need for an improved technique for accurate estimation of the blood PSD using considerably fewer Doppler transmissions. Since every sample in the slow-time signal is related to a certain pulse emission, we refer to the Doppler transmissions as slow-time samples.

In order to overcome these shortcomings, the authors in [2, 3, 4] proposed several approaches using deterministic and random sampling schemes. These include two iterative techniques, BIAA and BSLIM, which experimentally enable estimating the PSD using 30% of the transmissions usually used. In [5, 6] two approaches based on compressed sensing (CS) [7] were presented. However, all these previous methods are difficult for real-time implementation, due to their iterative nature. In addition, no analysis was performed on the minimal number of slow-time samples ensuring adequate reconstruction of the spectrum, using these techniques.

In this paper, we adopt recent work from the fields of MIMO radar and DOA estimation [8, 9] and propose an irregular sparse transmission scheme for blood spectral Doppler which we refer to as nested slow-time sampling. An analysis of the proposed approach is performed, showing that the minimal number of Doppler transmissions allowing spectrum reconstruction is proportional to the square root of P. We then present a computationally efficient estimator which exploits nested slow-time sampling and is shown, using realistic Field II simulation data [10], to outperform BIAA and BSLIM [2] by producing accurate estimation of the blood velocity from only 12% of the OW with size $P = 256$. This allows for updating the B-mode image at high rate and/or estimating the PSD of the blood at several regions of interest simultaneously while maintaining spectral and temporal resolution.

This paper is organized as follows. In Section 2, we present the blood scattering model and formulate our problem. Section 3 describes the nested slow-time sampling scheme and the proposed algorithm for spectrum reconstruction. In Section 4, we derive the minimal number of Doppler transmissions required by the nested approach. Numerical experiments are presented in Section 5.

2. SYSTEM MODEL AND PROBLEM FORMULATION

In spectral Doppler the ultrasound scanner transmits a pulse train

$$s_T(t) = \sum_{p=0}^{P-1} \sin\left(2\pi f_c \left(t - pT\right)\right), \; 0 \le t \le PT, \qquad (1)$$

This work was funded by the European Union's Horizon 2020 research and innovation program under grant agreement No. 646804-ERC-COG-BNYQ.

consisting of P equally spaced pulses $\sin(2\pi f_c t)$ where f_c is the center frequency of the signal. The pulse repetition interval is T, and its reciprocal $f_{prf} = 1/T$ is the pulse repetition frequency (PRF).

Consider a single blood scatterer. The noise-free received signal can be modeled as

$$s(t) = \sum_{p=0}^{P-1} \alpha \sin\left(2\pi f_c \left(t - pT - \frac{2d_p}{c}\right)\right), \tag{2}$$

where p is the emission number (slow-time sample index), c is the sound wave propagation speed, α is the amplitude related to the blood scatterer reflectivity and d_p is its depth. It will be convenient to express $s(t)$ as a sum of single frames $s(t) = \sum_{p=0}^{P-1} s_p(t)$, where

$$s_p(t) = \alpha \sin\left(2\pi f_c \left(t - pT - \frac{2d_p}{c}\right)\right). \tag{3}$$

The blood scatterer movement along the beam direction during P consecutive transmissions is given by

$$d_p = d_0 + vpT, \qquad 0 \le p \le P-1, \tag{4}$$

where d_0 is the initial depth of the blood scatterer and v is its axial velocity. Substituting (4) into (3), we get

$$s_p(t) = \alpha \sin\left(2\pi f_c \left(t - pT - \frac{2d_0}{c} - \frac{2v}{c}pT\right)\right). \tag{5}$$

We wish to recover the blood scatterer unknown axial velocity v and the variance of its amplitude α from the received signal $s(t)$. We begin by deriving an expression for the samples of $s(t)$ and show how v and α are embodied in them. To this end, each aligned frame $s_p(t + pT)$ is sampled yielding the discrete signal

$$s_p[k] = s_p\left(\frac{k}{f_s} + pT\right) = \alpha \sin\left(2\pi f_c \left(\frac{k}{f_s} - \frac{2d_0}{c} - \frac{2v}{c}pT\right)\right), \tag{6}$$

where f_s is the sampling frequency and k is the sample index associated with depth (fast-time sample index). For mathematical convenience, we rewrite the signal as a 2D function

$$s[k,p] = \alpha \sin\left(2\pi f_c \left(\frac{k}{f_s} - \frac{2d_0}{c} - \frac{2v}{c}pT\right)\right). \tag{7}$$

The analytical signal is then

$$x[k,p] = \alpha \exp\left(2\pi j f_c \left(\frac{k}{f_s} - \frac{2d_0}{c} - \frac{2v}{c}pT\right)\right). \tag{8}$$

Since f_c/f_s is known, we demodulate $x\,[k,p]$ resulting in

$$y\,[k,p] = \alpha \exp\left(-2\pi j f_c \left(\frac{2d_0}{c} + \frac{2v}{c}pT\right)\right). \tag{9}$$

Denoting the Doppler frequency by $\psi \triangleq -\frac{2v}{c} f_c T$, we have

$$y\,[k,p] = \widetilde{\alpha} \exp\left(2\pi j \psi p\right), \tag{10}$$

where we define $\widetilde{\alpha} = \alpha \exp\left\{-j\frac{4\pi f_c d_0}{c}\right\}$ to simplify notations.

In the general case, each resolution cell of the ultrasound system contains a distribution of scatterers. Consequently, the measured signal consists of M unknown frequencies $\{\psi_m\}_{m=1}^M$, each with corresponded velocity v_m. Taking the latter into account in addition to noise, we rewrite (10) as

$$y\,[k,p] = \sum_{m=1}^{M} \alpha_m e^{2\pi j \psi_m p} + w\,[k,p], \tag{11}$$

where α_m is a complex amplitude related to the number of scatterers with axial velocity v_m and $w[k,p]$ is zero mean white complex Gaussian noise with unknown variance σ^2 assumed to be uncorrelated with the amplitudes. The Doppler frequencies $\{\psi_m\}_{m=1}^M$ are assumed to lie in the unambiguous frequency domain, that is $|\psi_m| \le 1/2$, for all $1 \le m \le M$. We also assume that the amplitudes are statistically uncorrelated with unknown variances $\sigma_m^2 = \mathbb{E}[|\alpha_m|^2]$. Assembling the slow-time samples $y\,[k,p]$ for P consecutive transmissions into a vector we obtain

$$\mathbf{y}\,[k] = \mathbf{A}\boldsymbol{\alpha} + \mathbf{w}[k], \tag{12}$$

where $\mathbf{y}\,[k] = [y\,[k,0]\,...y\,[k,P-1]]^T \in \mathbb{C}^{P\times 1}$ is the slow-time vector and $\mathbf{w}[k]$ is the noise vector defined accordingly. The vector $\boldsymbol{\alpha} \in \mathbb{C}^{M\times 1}$ consists of M amplitudes $\{\alpha_m\}_{m=1}^M$ and $\mathbf{A} \in \mathbb{C}^{P\times M}$ is a Vandermonde matrix, whose pmth entry is given by $[\mathbf{A}]_{pm} = \exp(2\pi j \psi_m p)$. Our goal is to estimate from (12) the frequencies $\{\psi_m\}_{m=1}^M$ and the variances $\{\sigma_m^2\}_{m=1}^M$.

Define the autocorrelation matrices $\mathbf{R}_\alpha = \mathbb{E}\left[\boldsymbol{\alpha}\boldsymbol{\alpha}^H\right] \in \mathbb{R}^{M\times M}$ and $\mathbf{R}_\mathbf{y} = \mathbb{E}\left[\mathbf{y}[k]\mathbf{y}[k]^H\right] \in \mathbb{R}^{P\times P}$. Then from (12), we have

$$\mathbf{R}_\mathbf{y} = \mathbf{A}\mathbf{R}_\alpha\mathbf{A}^H + \sigma^2\mathbf{I}, \tag{13}$$

where $(\cdot)^H$ denotes the Hermitian conjugate. Since we assume the amplitudes are statistically uncorrelated, the matrix $\mathbf{R}_\alpha$ is a diagonal matrix with $\mathbf{R}_\alpha(m,m) = \sigma_m^2$. Denoting by $\mathbf{p} \in \mathbb{R}^{M\times 1}$ the diagonal of $\mathbf{R}_\alpha$, it follows that

$$\mathbf{z} = \mathrm{vec}(\mathbf{R}_\mathbf{y}) = \left(\mathbf{A}^* \odot \mathbf{A}\right)\mathbf{p} + \sigma^2\mathrm{vec}(\mathbf{I}), \tag{14}$$

where $(\cdot)^*$ denotes the conjugate and $\odot$ the Khatri-Rao product. We wish to recover the power spectrum vector $\mathbf{p}$ from (14). Note, however, that $\mathbf{A}$ is unknown.

In standard processing [1], the Doppler frequencies are assumed to lie on the Nyquist grid so that $\psi_m = 2\pi i_m/PT$, where i_m is an integer in the range $[0, P-1]$. This implies that (14) can be rewritten with $\mathbf{A} = \mathbf{F}^H \in \mathbb{C}^{P\times P}$ being scaled inverse fast Fourier transform (IFFT) matrix and $\mathbf{p} \in \mathbb{R}^{P\times 1}$ a vector that contains the value σ_m^2 at index i_m. In this case, the spectral resolution is equal to $2\pi/PT$, where P is chosen large enough to attain sufficient resolution. Assuming we have enough snapshots of the slow-time vector to estimate the autocorrelation matrix, the power spectrum $\mathbf{p}$ is conventionally estimated by applying FFT on each snapshot and averaging the squared magnitude of the result. A spectogram is a visual representation of the spectrum estimation $\mathbf{p}$ as it varies with time.

Our goal is to recover the power spectrum $\mathbf{p}$ with improved spectral resolution while significantly reducing the number of transmitted pulses, namely we sub-sample $\mathbf{y}[k]$. In the next sections, we show that we can reconstruct $\mathbf{p}$ with resolution of $2\pi/(2P-1)T$ while transmitting only $2\sqrt{P}$-1 pulses.

3. NESTED SAMPLING

3.1. Nested slow-time sampling

In this work, we propose sending only $N < P$ pulses with non-uniform time steps between them over the entire CPI. This way, by exploiting the periods of time where no pulse is sent in a certain direction, the same CPI is used for B-mode transmission sequences and several spectral Doppler transmissions in different directions.

Following [9], we introduce two integers $1 \le N_1, N_2 \le P$ such that $N_1 + N_2 = N < P$ where P is the size of the observation window. Given N_1 and N_2, we define the following two sets

$$\begin{aligned} S_{N_1} &= \{m-1, \qquad\quad m = 1,2,...,N_1\}, \\ S_{N_2} &= \{n\,(N_1+1)-1, \;\; n = 1,2,...,N_2\}, \end{aligned} \tag{15}$$

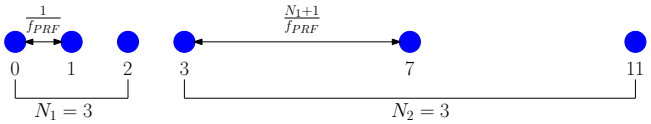

Fig. 1. **Nested transmission pattern.** $N_1 = N_2 = 3$ for an observation window of size $P = 12$. Every circle represents a Doppler pulse emission.

which are illustrated in Fig. 1. Next, we consider a non-uniform pulse train for spectral Doppler imaging such that the nth pulse is sent at time $p_n T$, where $S_N = \{p_n\}_{n=0}^{N-1}$ is the ordered set of the union of S_{N_1} and S_{N_2}. In this case, (1) becomes

$$s_T(t) = \sum_{n=0}^{N-1} \sin\left(2\pi f_c \left(t - p_n T\right)\right), \qquad 0 \le t \le PT. \tag{16}$$

Following the processing on the received signals described in Section 2, the measured signal can be written similarly to (11) as

$$y\left[k, n\right] = \sum_{m=1}^{M} \alpha_m e^{2\pi j \psi_m p_n}, \qquad 0 \le n \le N-1, \tag{17}$$

where we neglect the noise term. In vector form we have

$$\mathbf{y}_N[k] = \mathbf{A}_N \boldsymbol{\alpha}, \tag{18}$$

where $\mathbf{y}_N[k] \in \mathbb{C}^{N\times 1}$ is the nested slow-time vector composed of samples from N emissions and $\mathbf{A}_N \in \mathbb{C}^{N\times M}$ is a sub-matrix of the Vandermonde matrix $\mathbf{A}$ in (12), whose nmth entry is given by $[\mathbf{A}_N]_{nm} = \exp(2\pi j \psi_m p_n)$.

Denote the autocorrelation matrix $\mathbf{R}_{\mathbf{y}_N} = \mathbb{E}\left[\mathbf{y}_N[k]\mathbf{y}_N^H[k]\right] \in \mathbb{R}^{N\times N}$. Similar to (14), we have

$$\mathbf{z}_N = vec(\mathbf{R}_{\mathbf{y}_N}) = \left(\mathbf{A}_N^* \odot \mathbf{A}_N\right)\mathbf{p}, \tag{19}$$

where $(\mathbf{A}_N^* \odot \mathbf{A}_N) \in \mathbb{C}^{N^2\times M}$ and $\mathbf{p} \in \mathbb{R}^{M\times 1}$. Define the difference set of S_N as $D_S = \{p_j - p_i,\ 0 \le i, j \le N-1\}$. Then, the matrix $\mathbf{A}_N^* \odot \mathbf{A}_N$ has dmth entry $\exp\left(2\pi j \psi_m D_S(d)\right)$.

The system defined in (19) is overdetermined for $N^2 \ge M$, if $(\mathbf{A}_N^* \odot \mathbf{A}_N)$ is full column rank. The following theorem, whose proof can found in [9], provides the condition for this system to have a unique solution.

Theorem 1. *Let $\mathbf{A}_N \in \mathbb{C}^{N\times M}$ be the matrix defined in (18) with $|\psi_m| \le 1/2$. Then, the matrix $(\mathbf{A}_N^* \odot \mathbf{A}_N) \in \mathbb{C}^{N^2\times M}$ has $2N_2(N_1+1) - 1$ distinct rows. It is full column rank if $2N_2(N_1+1) - 1 \ge M$.*

The number of distinct rows of $(\mathbf{A}_N^* \odot \mathbf{A}_N)$ is equal to the number of distinct elements in D_S. The authors in [9] prove that for the choice of S_N given here, the difference set has exactly $2N_2(N_1+1) - 1$ distinct elements. Following Theorem 1, (19) has a unique solution if $2N_2(N_1+1) - 1 \ge M$. In order to preserve the overall CPI, N_1 and N_2 are chosen such that $N_2(N_1+1) = P$. This implies that if the statistics can be estimated then perfect recovery of the blood power spectrum $\mathbf{p}$, transmitting only $N < P$ pulses, is guaranteed for $2P > M$.

3.2. Spectrum reconstruction

We now provide a fast method to reconstruct the blood power spectrum $\mathbf{p}$ from slow-time samples obtained using nested sampling.

First, we approximate the autocorrelation matrix $\hat{\mathbf{R}}_{\mathbf{y}_N}$ by using samples $\mathbf{y}_N[k]$ over neighboring depths $k = k_1, ..., k_K$

$$\hat{\mathbf{R}}_{\mathbf{y}_N} = \frac{1}{K}\sum_{k=k_1}^{k_K} \mathbf{y}_N\left[k\right]\mathbf{y}_N^H\left[k\right]. \tag{20}$$

Algorithm 1 Nested Blood Doppler (NBD)

Input: Nested slow-time vectors $\{\mathbf{y}\left[k\right]\}_{k=k_1}^{k=k_K}$, thresholding parameter $\lambda > 0$.
Output: Blood Doppler spectrum vector $\mathbf{p}$.
1: Estimate $\hat{\mathbf{R}}_{\mathbf{y_N}}$ using (20) and compute $\mathbf{z}_N = \text{vec}(\hat{\mathbf{R}}_{\mathbf{y_N}})$
2: Form $\mathbf{z}_1$ by averaging
3: Compute $\hat{\mathbf{p}} = \frac{1}{2P-1}\text{FFT}(\mathbf{z}_1)$
4: Perform soft-thersholding $\mathbf{p} = \mathcal{T}_\lambda\left(\hat{\mathbf{p}}\right)$.

Algorithm 2 Smooth Nested Blood Doppler (SNBD)

Input: Nested slow-time vectors $\{\mathbf{y}_N\left[k\right]\}_{k=k_1}^{k=k_K}$, smoothing and thresholding parameters $\mu > 0$ and $\lambda > 0$, smoothing matrix $\mathbf{Q}$.
Output: Blood Doppler spectrum vector $\mathbf{p}$.
1: Estimate $\hat{\mathbf{R}}_{\mathbf{y_N}}$ using (20) and compute $\mathbf{z}_N = \text{vec}(\hat{\mathbf{R}}_{\mathbf{y_N}})$
2: Form $\mathbf{z}_1$ by averaging
3: Compute $\hat{\mathbf{p}} = \frac{1}{2P-1}\text{FFT}\left((\mathbf{I} + \mu\mathbf{Q})^{-1}\mathbf{z}_1\right)$
4: Perform soft-thersholding $\mathbf{p} = \mathcal{T}_\lambda\left(\hat{\mathbf{p}}\right)$.

Since the autocorrelation is estimated from a finite number of snapshots, (19) is only satisfied approximately. In addition, we consider additive noise, so that (19) becomes

$$\mathbf{z}_N = \text{vec}(\hat{\mathbf{R}}_{\mathbf{y_N}}) = \left(\mathbf{A}_N^* \odot \mathbf{A}_N\right)\mathbf{p} + \sigma^2\text{vec}(\mathbf{I}), \tag{21}$$

where σ^2 is the noise as in Section 2.

We define D_u as the ordered set of the unique elements of D_S. We then construct a new matrix $\mathbf{A}_1 \in \mathbb{C}^{2P-1\times M}$ from $\mathbf{A}_N^* \odot \mathbf{A}_N$ where we remove the repeated rows and sort them so that the nth row corresponds to the nth element in D_u. Accordingly, we average the corresponding rows from $\mathbf{z}_N$ to get

$$\mathbf{z}_1 = \mathbf{A}_1\mathbf{p} + \sigma^2\tilde{\mathbf{e}}, \tag{22}$$

where $\tilde{\mathbf{e}} \in \mathbb{R}^{2P-1\times 1}$ is all zeros except a 1 at the Pth position.

Suppose now we limit ourselves to the Nyquist grid so that $\psi_m = 2\pi i_m/(2P-1)T$, where i_m is an integer in the range $0 \le i_m \le 2P-2$. In this case, $\mathbf{A}_1 = \mathbf{F}^H \in \mathbb{C}^{2P-1\times 2P-1}$ is scaled IFFT matrix. Therefore, we apply a scaled FFT on (22) to get

$$\hat{\mathbf{p}} = \frac{\mathbf{F}\mathbf{z}_1}{2P-1} = \frac{\mathbf{F}(\mathbf{F}^H\mathbf{p} + \sigma^2\tilde{\mathbf{e}})}{2P-1} = \mathbf{p} + \frac{\sigma^2}{2P-1}\mathbf{1}, \tag{23}$$

where $\mathbf{F}$ is the FFT matrix and $\mathbf{1} \in \mathbb{R}^{2P-1\times 1}$ is a vector of all ones. Finally, we estimate the power spectrum $\mathbf{p}$ by removing the noise variance from $\hat{\mathbf{p}}$ through soft-thresholding defined as $\mathcal{T}_\lambda(x) = \max(x-\lambda, 0)$ for a suitable choice of λ. The proposed technique is outlined in Algorithm 1, referred to as NBD.

Often, the power spectrum is assumed to be smooth. Rather than performing smoothing as part of post-processing, we instead formulate a least squares problem with a quadratic regularization functional that imposes smoothness on the power spectrum

$$\min_{\mathbf{p}} \left\|\mathbf{z}_1 - \mathbf{F}^H\mathbf{p}\right\|_2^2 + \mu\left\|\mathbf{D}\mathbf{p}\right\|_2^2, \tag{24}$$

where $\mu \in \mathbb{R}$ is a smoothing parameter and $\mathbf{D} \in \mathbb{R}^{2P-1\times 2P-1}$ is a circulant matrix where the first row is all zeros except a 1 and -1 on the first and second entries respectively, and each row is a right cyclic shift of the preceding row. The solution of (24) is given by

$$\hat{\mathbf{p}}_{smooth} = \left(\mathbf{F}\mathbf{F}^H + \mu\mathbf{D}^H\mathbf{D}\right)^{-1}\mathbf{F}\mathbf{z}_1. \tag{25}$$

The matrix $\mathbf{D}^H\mathbf{D}$ is also circulant, hence, it is diagonalized by the FFT matrix, i.e, $\mathbf{D}^H\mathbf{D} = \mathbf{F}\mathbf{Q}\mathbf{F}^H$ where $\mathbf{Q} \in \mathbb{R}^{2P-1\times 2P-1}$ is a diagonal matrix with $\mathbf{Q}(i,i) = \frac{2-2\cos(2\pi i/(2P-1))}{2P-1}$. Taking the latter into consideration, the solution can be simplified to

$$\hat{\mathbf{p}}_{smooth} = \left(\mathbf{F}\mathbf{F}^H + \mu\mathbf{F}\mathbf{Q}\mathbf{F}^H\right)^{-1}\mathbf{F}\mathbf{z}_1 = \frac{\mathbf{F}(\mathbf{I}+\mu\mathbf{Q})^{-1}\mathbf{z}_1}{2P-1}. \tag{26}$$

Again, we perform soft-thresholding on $\hat{\mathbf{p}}_{smooth}$ to estimate $\mathbf{p}$. This recovery method is summarized in Algorithm 2, referred to as SNBD. Note that Algorithm 2 reduces to Algorithm 1 for $\mu = 0$, hence, it can be viewed as a generalization of Algorithm 1 where we apply a smoothing window on $\mathbf{z}_1$ before performing FFT.

The complexity of the proposed methods is $\mathcal{O}(N^2 + P\log P)$, making them suitable for real-time estimation of the spectrum with improved resolution of $2\pi/(2P-1)T$ from fewer transmissions.

4. MINIMAL SAMPLING RATE

We next derive the minimal number of transmissions that can be achieved using the nested sampling introduced in Section 3.

Recall that the number of emissions is given by $N = N_1 + N_2$ under the constraint that $N_2(N_1+1) = P$. We, therefore, formulate the next optimization problem

$$\min_{N_1,N_2} N_1 + N_2 \; s.t. \; N_2\left(N_1+1\right) = P. \tag{27}$$

Using the inequality of arithmetic and geometric means, we bound the objective function from below by

$$(N_1 + 1 + N_2) - 1 \geq 2\sqrt{N_2(N_1+1)} - 1 = 2\sqrt{P} - 1. \tag{28}$$

This lower bound is obtained for $N_1 = \sqrt{P}-1,\; N_2 = \sqrt{P}$, making them the optimal solution of (27). Thus, the minimal number of slow-time samples required is $N = 2\sqrt{P} - 1$.

The desired spectral resolution of the estimation determines the size P of the OW. Thereby, the last result implies that when an OW of size P is required, the blood power spectrum can be reconstructed using only $\Theta(\sqrt{P})$ Doppler emissions. For example, given an observation window with $P = 256$, the blood power spectrum can be recovered using 31 pulses, which is only 12% of the OW, far less than 30% previously proposed by state-of-the-art methods.

5. NUMERICAL EXPERIMENTS

We now proceed to demonstrate blood PSD reconstruction from nested slow-time samples. The algorithms proposed in Section 3 were compared to BIAA and BSLIM, which were applied directly on the slow time vectors $y_N[k]$ to estimate the PSD iteratively. Realistic flow data was simulated using the Field II program with the Womersley model [10] for pulsating flow from the femoral artery. The autocorrelation matrix was estimated using $K = 33$ regularly spaced samples along depth. The PRF was set to 5 kHz for a mean velocity of 0.1 m/s and a beam/flow angle of 60°. The transducer had a center frequency of 3.5 MHz. An OW of size $P = 256$ was selected with $N_1 = 15$ and $N_2 = 16$ for the nested sampling. The thresholding parameter λ for both NBD and SNBD was chosen adaptively as 0.5 of the maximum of $\hat{\mathbf{p}}$ given by stage 3 in both algorithms. For SNBD a smoothing parameter $\mu = 0.1$ was used.

The resulting spectograms are shown in Fig. 2. We see clearly that Welch's method, BIAA and BSLIM suffer from substantially more artifacts, mainly because of aliasing. NBD and SNBD both produce a clear spectogram where the result of the latter is smoother, as expected. Additional simulations, which are not present due to lack of space, emphasizes the superiority of the proposed algorithms when the observation window is taken to be smaller.

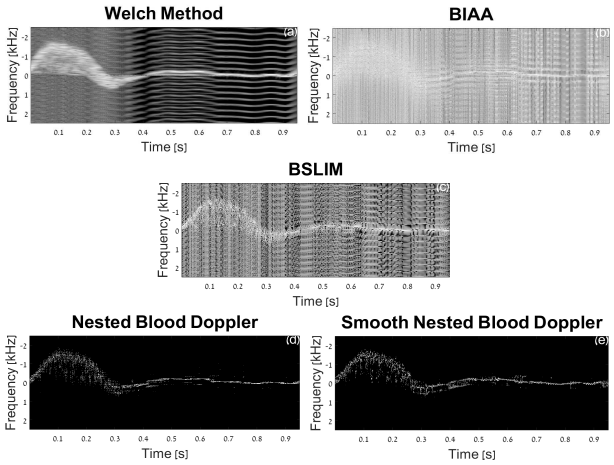

Fig. 2. **Comparison results.** (a) Welch's spectogram (b) BIAA spectogram (c) BSLIM spectogram (d) NBD spectogram (e) Smooth NBD spectogram. All spectograms were normalized to have a dynamic range of 60 dB.

6. CONCLUSION

In this paper, we introduced a new irregular sampling scheme for slow-time emissions. An analysis of the minimal number of transmissions required using the proposed approach revealed that the power spectrum can be reconstructed with enhanced resolution from a precedential small number of Doppler pulses. This offers a mode where several blood regions can be interrogated simultaneously while still updating the B-mode image at a high frame rate. A fast recovery algorithm, based on the sparse emission pattern presented, was derived and verified using Field II data to produce adequate spectograms, outperforming current state-of-the-art methods, while using much fewer pulses.

7. REFERENCES

[1] P. D. Welch, "The use of fast Fourier transform for the estimation of power spectra: A method based on time averaging over short, modified periodograms," *IEEE Trans. Audio and Electroacoustics*, vol. 15, no. 2, pp. 70–73, 1967.

[2] E. Gudmundson, A. Jakobsson, J. A. Jensen, and P. Stoica, "Blood velocity estimation using ultrasound and spectral iterative adaptive approaches," *Signal Process.*, vol. 91, no. 5, pp. 1275–1283, 2011.

[3] J. A. Jensen, "Spectral velocity estimation in ultrasound using sparse data sets," *Acoustical Society of America. Journal*, vol. 120, no. 1, pp. 211–220, 2006.

[4] S. K. Mollenbach and J. A. Jensen, "Duplex scanning using sparse data sequences," in *IUS 2008*. IEEE, 2008, pp. 5–8.

[5] J. Richy, D. Friboulet, A. Bernard, O. Bernard, and H. Liebgott, "Blood velocity estimation using compressive sensing," *IEEE Trans. on Medical Imaging*, vol. 32, no. 11, pp. 1979–1988, 2013.

[6] O. Lorintiu, H. Liebgott, and D. Friboulet, "Compressed sensing doppler ultrasound reconstruction using block sparse bayesian learning," *IEEE Trans. on Medical Imaging*, vol. 35(4), pp. 978–987, 2016.

[7] Y. C. Eldar and G. Kutyniok, *Compressed sensing: theory and applications*, Cambridge University Press, 2012.

[8] P. Pal and P. P. Vaidyanathan, "A novel array structure for directions-of-arrival estimation with increased degrees of freedom," in *ICASSP*. IEEE, 2010, pp. 2606–2609.

[9] P. Pal and P. P. Vaidyanathan, "Nested arrays: A novel approach to array processing with enhanced degrees of freedom," *IEEE Trans. Signal Process.*, vol. 58, no. 8, pp. 4167–4181, 2010.

[10] J. A. Jensen, "Field: A program for simulating ultrasound systems," *Med. Biol. Eng. Comput.*, vol. 34, no. 1, pp. 351–353, 1996.